The impact of parasitoid emergence time on host–parasitoid population dynamics

Christina A. Cobbold [a,b,*], Jens Roland [c], Mark A. Lewis [c,b]

[a] Department of Mathematics, University of Glasgow, Glasgow, Scotland G12 8QW, United Kingdom
[b] Department of Mathematics and Statistical Science, University of Alberta, Edmonton, Alberta, T6G 2G1, Canada
[c] Department of Biological Sciences, University of Alberta, Edmonton, Alberta, T6G 2G1, Canada

ARTICLE INFO

ABSTRACT

We investigate the effect of parasitoid phenology on host–parasitoid population cycles. Recent experimental research has shown that parasitized hosts can continue to interact with their unparasitized counterparts through competition. Parasitoid phenology, in particular the timing of emergence from the host, determines the duration of this competition. We construct a discrete-time host–parasitoid model in which within-generation dynamics associated with parasitoid timing is explicitly incorporated. We found that late-emerging parasitoids induce less severe, but more frequent, host outbreaks, independent of the choice of competition model. The competition experienced by the parasitized host reduces the parasitoids' numerical response to changes in host numbers, preventing the 'boom-bust' dynamics associated with more efficient parasitoids. We tested our findings against experimental data for the forest tent caterpillar (*Malacosoma disstria* Hübner) system, where a large number of consecutive years at a high host density is synonymous with severe forest damage.

1. Introduction

The timing of parasitoid emergence can impact the dynamics of parasitoid populations. This impact may be due to variable environmental factors that change between different possible parasitoid emergence times. However, a more subtle possibility arises. Emergence timing (also referred to as emergence phenology) may affect nonlinear host–parasitoid interaction dynamics. In particular, as we show below, late emerging parasitoids may experience environments of heightened within-host competition, and these in turn can affect the long-term parasitoid population dynamics.

Those parasitoids most susceptible to the impact of emergence timing on within-host competition dynamics are so-called koinobionts, parasitoids that do not kill their host immediately upon entry. This common form of parasitism allows hosts to continue feeding and developing until a later stage, whereupon the host is consumed and the parasite emerges. Because the impacts of within-host competition increase over time, late-emerging koinobionts run a heightened risk of mortality arising from their host succumbing to the within-host competition.

Experimental studies have shown competition occurs between both parasitized and unparasitized hosts. A study of the Indian meal moth system by Cameron et al. (2005) found that competition and mortality of unparasitized hosts was increased by the presence of parasitized hosts. Parasitism, itself, may affect the competitive ability of a host, as shown by Sisterson (2003)'s study of cranberry fruitworm, *Acrobasis vaccinii* Riley, parasitized by the hymenopteran parasitoid *Phanerotoma franklini* Gahan. In both studies, interactions are koinobiont. The parasitized hosts are not functionally dead, and the interaction between parasitized and unparasitized hosts ended only when the parasitoid emerged from the host.

Discrete-time models are suitable for natural insect systems from temperate climates that exhibit non-overlapping generations and enter diapause to overwinter. This is because the temperature-driven diapause has the effect of synchronizing the developmental clock of the population. Despite awareness that age structure and the specific host stage attacked by the parasitoid are important factors in determining the persistence of an introduced parasitoid (Godfray and Waage, 1991), there has been limited theoretical investigation into parasitoid emergence timing for discrete-time models. Even though discrete-time systems are well suited to describing diapausing populations, explicit descriptions of emergence phenology in this framework are missing from the literature. Those investigations made for discrete-time models have the simplifying assumption that parasitism occurs either before or after host competition (Wang and Gutierrez, 1980; May et al., 1981; Umbanhowar and Hastings, 2002), not during competition.

To date, explicit descriptions of phenology have largely been limited to continuous-time stage-structured models, which are

* Corresponding author at: Department of Mathematics, University of Glasgow, Glasgow, Scotland G12 8QW, United Kingdom.
E-mail addresses: cc@maths.gla.ac.uk (C.A. Cobbold), jroland@ualberta.ca (J. Roland), mlewis@math.ualberta.ca (M.A. Lewis).

ideal for describing insects whose generations overlap, but not for diapausing insects. Continuous-time stage-structured models for the timing of density-regulating events start with the pioneering work of Gurney et al. (1983). This work has been extended to include asymmetry in host density-dependence across host stages (Wearing et al., 2004; Briggs et al., 2000), parasitoid species which attack different host stages (Briggs, 1993; Briggs et al., 1993) and competition between parasitized hosts (Spataro and Bernstein, 2004). Most recently, White et al. (2007) included inter-class competition between the parasitized and unparasitized hosts. The host–parasitoid population dynamics were dramatically affected by the competition, which stabilized the interaction but in some cases induced parasitoid extinction.

In this paper we explore the effects of parasitoid phenology and inter-class competition in a discrete-time framework. Of particular interest is how these mechanisms impact the host population cycles that are commonplace in the natural world. We extend the ideas of Wang and Gutierrez (1980), May et al. (1981) and Umbanhowar and Hastings (2002), and explicitly model within-season parasitoid phenology by describing when a parasitoid emerges from a parasitized host. Competition for resources induces mortality of hosts, so we hypothesize that later-emerging parasitoids experience prolonged competition and a reduction in numbers compared to their early-emerging counterparts. We expect that later parasitoid emergence stabilizes the host–parasitoid dynamics. We investigate this effect of phenology on competition for a variety of competition models: specifically, we ask how emergence time affects the characteristics of host–parasitoid population cycles.

In Section 2 we derive a general description of parasitoid phenology by allowing competitive mortality of parasitized hosts. The focus of the analysis (Section 3) is to understand how oscillations in the host–parasitoid population are affected by parasitoid phenology. In particular, we look at the stabilizing effects of late parasitoid emergence and analyze the duration and frequency of host outbreaks as a function of parasitoid phenology. Finally, in Section 4, we validate the model against time series data for the forest tent caterpillar system and discuss the implications of parasitoid phenology for biological control.

2. The model

There have been many extensions of the original host–parasitoid model by Nicholson and Bailey (1935), exploring mechanistic descriptions of parasitism and host regulation in both spatial and non-spatial contexts (see Hassell (2000, 1978) for reviews). We present a generalization that focuses on explicitly describing parasitoid phenology, which has often been overlooked in discrete-time models. Parasitoid emergence time determines the duration of competition between parasitized and unparasitized hosts, and we explore the effects of parasitoid emergence time under a range of competition models.

Astrom et al. (1996) and Rodriguez (1988) derived an example of phenologically explicit single-population discrete-time model. They partitioned the within-season dynamics into a series of 'self-regulating' events and demonstrated that complex dynamics can emerge from such models, including the creation of multiple equilibria. We now extend these ideas to a multi-species system.

The general model that we present below has two extreme scenarios:

(1) Parasitoids emerge from the host prior to density-dependent competition. In this case there is no competition between parasitized and unparasitized hosts.
(2) The period of density-dependent competition between hosts is followed by parasitoid emergence. In this case, parasitized hosts experience the maximum amount of competition in a season.

Scenario (1) assumes that parasitized hosts are functionally dead. Examples are common in the literature and were first studied by Beddington et al. (1975). A special case of (2) was addressed by Wang and Gutierrez (1980), using a model developed further by May et al. (1981). Parasitism following density-dependence in the host life cycle was found to slightly reduce the stability of the host–parasitoid population dynamics, and equilibrium host densities were higher. Despite these early results, the study of phenology in discrete-time models has been largely neglected in the literature.

The model presented below allows us to consider the details of parasitoid phenology. Competition between parasitized and unparasitized hosts is described by a general functional form that allows us to explore the effects of both contest and scramble competition.

$$H_{t+1} = H_t \times \overbrace{e^r}^{\substack{\text{Intrinsic} \\ \text{growth}}} \times \overbrace{e^{-\mu(H_t)}}^{\substack{\text{Fraction of hosts} \\ \textbf{surviving density-dependence}}} \times \overbrace{f(P_t)}^{\substack{\text{Fraction of hosts} \\ \textbf{surviving parasitism}}} \quad (1a)$$

$$P_{t+1} = H_t \times \overbrace{e^{-\alpha\mu(H_t)}}^{\substack{\text{Fraction of parasitised hosts} \\ \text{surviving density-dependence}}} \times \overbrace{(1 - f(P_t))}^{\substack{\text{Fraction of hosts} \\ \text{parasitized}}} . \quad (1b)$$

In the model, H_t denotes the host density in year t and P_t the corresponding parasitoid density. The probability of a host evading parasitism is given by the zeroth term of the negative binomial, $f(P_t) = (1 + aP_t/\kappa)^{-\kappa}$ (May, 1978). Here a describes the searching efficiency of the parasitoid and $1/\kappa$ is the variance in host risk to parasitism. The parameter κ allows us to consider clumped parasitoid searching ($\kappa < 1$) and random searching ($\kappa \to \infty$). In the limit as $\kappa \to \infty$, we obtain the zeroth term of the Poisson distribution for the probability of evading parasitism ($f(P_t) = e^{-aP_t}$).

The parameter α describes parasitoid phenology and ranges between 0 and 1, depending on the stage in the parasitized host's development from which the parasitoid emerges. The timing of events in the host and parasitoid life cycles affects the survival of both species. We use the host life cycle as a reference point and model the timing of parasitism relative to the host. We assume that parasitized and unparasitized hosts compete for resources in functionally the same way. Therefore, density-dependent mortality of parasitized hosts is given by the term $e^{-\alpha\mu(H_t)}$. The density-dependent mortality of hosts affects parasitoids in two ways, reducing the number of host targets and inducing the death of parasitized hosts. Both reduce the potential number of new parasitoids. So parasitoid phenology can be described using parasitoid emergence time, and we can ignore the timing of the initial parasitoid attack in our single parasitoid model. However, the timing of attack becomes important if we consider a multi-parasitoid system, when competing parasitoid species need to locate unparasitized hosts.

In Section 2.1 we explicitly describe the within-season dynamics to explain our choice of the term to describe parasitoid mortality $e^{-\alpha\mu(H_t)}$.

2.1. Within-season dynamics

Bellows (1981) derived a general form for density-dependence, $e^{-\mu(H_t)}$, from a differential equation that describes within-season host dynamics,

$$\frac{dH}{dt} = -H\mu(H_0), \quad (2)$$

where $\mu(H_0)$ relates mortality rate of the host population to the initial host density, H_0. Solving (2) at $t = 1$ (scaled season length) gives the equation for hosts surviving one season of density-dependent mortality, and formulated as a difference equation gives

$$H_{t+1} = H_t \exp(-\mu(H_t)). \quad (3)$$

Table 1
Using maximum likelihood, seven models for host density-dependence, $\exp(-\mu(H_t))$, are fitted to the data described in Appendix B.1. Parameter estimates are given in the table together with the standard deviation of the error, $\hat{\sigma}$. Corrected AIC is calculated for all models, the lowest value indicating the most parsimonious model.

Entry	$\mu(H) = k$-value	Sign of $d^2\mu/dH^2$	$\hat{b}$	$\hat{c}$	$\hat{\sigma}$	AICc
1	$b \ln H$	$-$	0.94		0.74	26.67
2	cH	0		0.73	0.17	-1.71
3	$\ln(1 + cH)$	$-$		2.21	0.23	4.25
4	cH^b	$+-$	1.37	0.53	0.16	0.75
5	$\ln(1 + (cH)^b)$	$+-$	2.90	0.74	0.18	2.93
6	$b \ln(1 + cH)$	$-$	69.00	0.01	0.17	1.87
7	$\ln(1 + \exp(bH - c))$	$+$	1.21	1.38	0.15	-0.94

Table 1 lists seven mortality functions $\mu(H_t)$ discussed by Bellows. This formulation for density-dependence has the benefit that $\mu(H_t)$ can be measured empirically (Haldane, 1949; Varley and Gradwell, 1960).

The fraction of parasitized hosts surviving density-dependence is found by using the host life cycle as a reference point and partitioning the within-season events according to host life-stage. We assume that the host's life cycle consists of n non-overlapping stages. Let τ_i be the duration of stage i, and $T = \sum_{i=1}^{n} \tau_i$ be the duration of the host life cycle. Finally, since competition for resources may be stage-dependent, we introduce a mortality function $\mu_i(t)$ for hosts in stage i.

The number of host eggs at the start of the season is H_t, and τ_1/T denotes the proportion of the season that hosts are in the first developmental stage. Solving Eq. (2) at the scaled time τ_1/T gives $H_t \exp(-\mu_1(H_t)(\frac{\tau_1}{T}))$ hosts surviving to the end of the first stage. The number of hosts surviving to the end of stage n is therefore given by

$$H_t e^{-\mu_1(H_t)\frac{\tau_1}{T}} e^{-\mu_2(H_t)\frac{\tau_2}{T}} \ldots e^{-\mu_n(H_t)\frac{\tau_n}{T}} = H_t e^{-\frac{1}{T}(\sum_{i=1}^{n} \tau_i \mu_i(H_t))}$$
$$= H_t e^{-\mu(H_t)}.$$

The seasonal mortality function, $\mu(H_t) = \frac{1}{T}(\sum_{i=1}^{n} \tau_i \mu_i(H_t))$, is a weighted average of the mortality functions acting at each stage of the host life cycle.

To model the effect of density-dependence on parasitoids, we assume that parasitized and unparasitized hosts compete equally for resources. A parasitoid survives to emerge from a host in stage L provided the parasitized host has survived competition until stage L. The number of hosts surviving density-dependence to reach the end of the Lth stage is given by

$$H_t e^{-\frac{1}{T}(\sum_{i=1}^{L} \tau_i \mu_i(H_t))} = H_t e^{-\alpha\mu(H_t)},$$

where

$$\alpha = \frac{\sum_{i=1}^{L} \tau_i \mu_i(H_t)}{\sum_{i=1}^{n} \tau_i \mu_i(H_t)} = \frac{\frac{1}{T}\sum_{i=1}^{L} \tau_i \mu_i(H_t)}{\mu(H_t)}. \qquad (4)$$

In this general case, $\mu_i(H_t)$ may differ for each stage.

In the simple case of $\mu_i(H_t) = \mu(H_t)$ for all i we can define α by

$$\alpha = \frac{1}{T} \sum_{i=1}^{L} \tau_i.$$

This expression also holds if density-dependence only affects particular stages of the host life cycle, in which case T is interpreted as the duration of the density-dependent period and, as before, α is the proportion of the density-dependent season experienced by the parasitized host.

In the example of Ricker density-dependence acting at each stage, but with a stage-dependent carrying capacity, the expression for α can be shown to be independent of H_t. The stage-dependent mortality is given by $\mu_i(H_t) = rH_t/K_i$, where K_i is the

carrying capacity of the ith stage and r is the intrinsic host growth rate. Eq. (4) yields

$$\alpha = \frac{\sum_{i=1}^{L} \tau_i \frac{rH_t}{K_i}}{\sum_{i=1}^{n} \tau_i \frac{rH_t}{K_i}} = \frac{K}{T} \sum_{i=1}^{L} \tau_i/K_i,$$
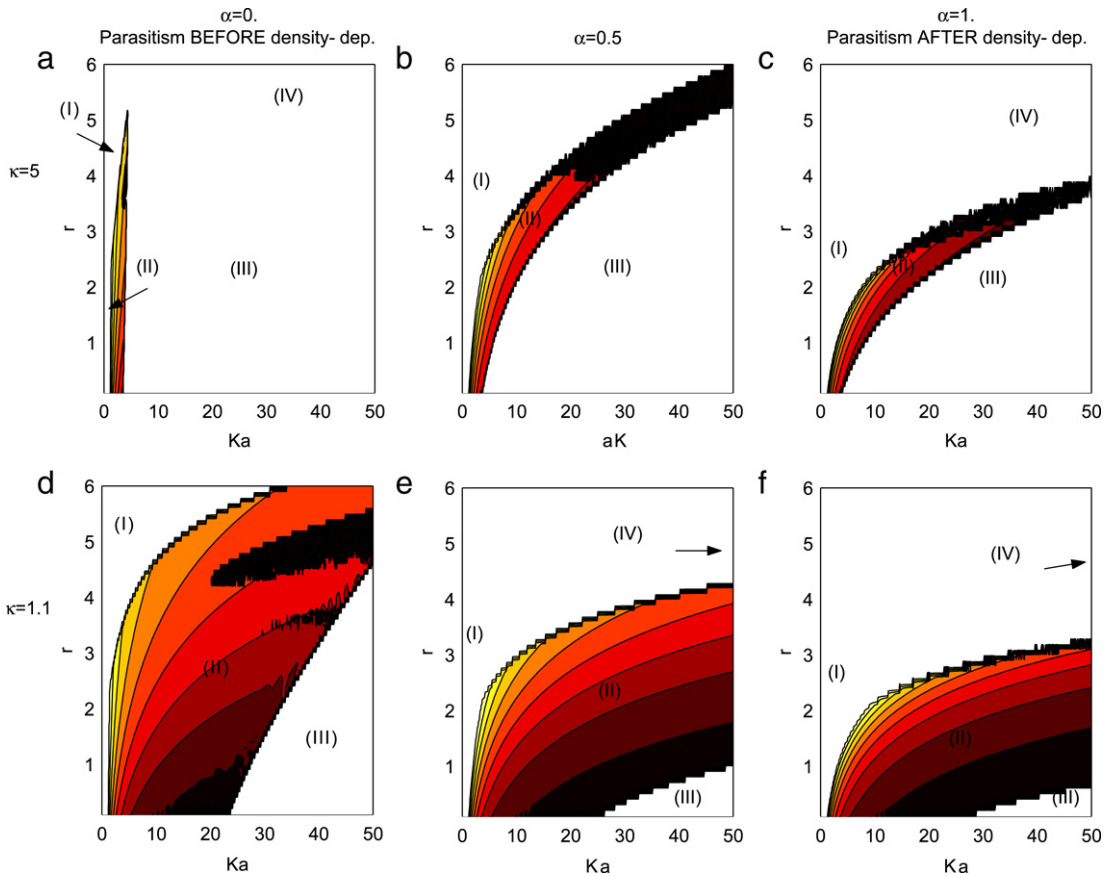
where $K = T/(\sum_{i=1}^{n} \frac{\tau_i}{K_i})$ is the seasonal carrying capacity and is a weighted harmonic mean of the K_is. In this case the seasonal mortality function is given by $\mu(H_t) = rH_t/K$.

In this paper we focus on the simplified case where $\mu_i(H_t) = \mu(H_t)$ for each density-dependent life stage i. The special case of the model Eqs. (1) where $\mu(H_t) = r(H_t/K)^b$ was considered by Berstein (1986) and Taylor (1997). The range of α in the Bernstein and Taylor models is unconstrained, allowing for parasitized hosts to be more susceptible to competition than their unparasitized counterparts. Their work focused on the stability properties of the model; they found that increasing α increased the region of stable coexistence and depressed host density. The objective of our work is to study the host–parasitoid population cycles, investigating how α affects the characteristics of these cycles under a range of models for host competition. This gives insight into how parasitoid phenology may impact on host outbreaks.

3. Results

The general model given by Eqs. (1) has three equilibria: extinction of both host and parasitoid, host-only persistence, and coexistence. In the absence of parasitoids, the host persists at a stable equilibrium H^* if $r > \mu(0)$. When $\mu'(H^*)H^* > 2$, the host-only equilibrium becomes unstable via a period-doubling bifurcation giving rise to regular cycles of period 2. Lastly, stable limit cycles can exist when the host–parasitoid coexistence equilibrium becomes unstable.

We now focus our attention on the existence of stable limit cycles. Both the choice of parasitism function and host density-dependence are known to affect the stability of the coexistence equilibrium. Clumped parasitism ($f(P_t)$ with $\kappa < 1$) and host contest competition (e.g. $\mu(H_t) = r(H_t/K)^b$, with $b < 1$) increase equilibrium stability and reduce the prevalence of population cycles. To study how α affects the prevalence of host–parasitoid population cycles, we need to fix our choice of density-dependence. We take $\mu(H) = rH_t/K$ and keep the more general form of parasitism described by the negative binomial. The Jury conditions are then used to construct stability boundaries separating regions of $r - (aK)$ parameter space (Neubert and Kot, 1992). Columns 1 through 3 of Fig. 1 illustrate the boundaries for the three values of α: 0 (early larval parasitoids), 0.5 (late larval parasitoids) and 1 (pupal parasitoids). The first row of plots shows the large value

Fig. 1. $r - (aK)$ parameter-plane describing the stability of the host–parasitoid coexistence equilibrium for Eq. (1), with $\mu(H_t) = rH_t/K$ and $f(P_t) = (1 + aP_t/\kappa)^{-\kappa}$. The degree of parasitoid clumping is given by κ, and aK provides a scaled measure of parasitoid searching efficiency. Columns from left to right indicate increasing α, the rows from top to bottom decreasing κ. The regions labeled (I)–(IV) indicated different host–parasitoid dynamics: (I) parasitoid extinction, (II) equilibrium host–parasitoid coexistence, (III) stable population cycles, (IV) chaotic behavior. The shading in the stable coexistence region (II) indicates $q = H^*/K$, the extent to which the host equilibrium is depressed below the carrying capacity K. The light shading corresponds to $q \approx 1$ and the dark shading corresponds to $q \approx 0$.

$\kappa = 5$, random type searching. The second row shows the small value $\kappa = 1.1$, clumped searching. Reducing κ increases the stability of the model, thereby increasing the size of region (II), stable host–parasitoid coexistence.

For small host growth rates, late parasitoid emergence increases the stability of the coexistence equilibrium. For large host growth rates, coexistence is lost frequently, giving way to parasitoid extinction or chaos. Stable coexistence of the host with a late-emerging parasitoid requires a low host growth rate, which limits density-dependent mortality of parasitized hosts. Parasitoids emerging later require a greater number of hosts for replacement, which makes them more vulnerable to extinction, but can also allow the parasitoid to persist with the host even when the parasitoid is an overly efficient searcher (corresponding to large values of a).

The shading in Fig. 1 denotes the value of $q = H^*/K$, the extent to which the parasitoid depresses the host below its carrying capacity. Light indicates $q \approx 1$ and dark corresponds to $q \approx 0$. Early-emerging parasitoids depress the host more than late-emerging parasitoids, when all other parameters are fixed. However, the shading in Fig. 1 also shows that as α increases, the region of parameter space associated with low host density (dark shading) increases. So host density is more sensitive to parameter changes when the host coexists with an early-emerging parasitoid.

Berstein (1986) considered local stability boundaries for the case where $\mu(H_t) = r(H_t/K)^b$. Reducing b below 1 expanded the region of stable coexistence and increased host levels. The mortality function when $b < 1$ corresponds to contest competition, and Bellows (1981) showed that many of the other models of competition can be derived from this mortality function.

3.1. Analysis of the consumer–resource cycles

The remainder of the paper focuses on the consumer–resource population cycles found in region (III) of Fig. 1. We demonstrate that the cycle descriptors (period, outbreak duration, etc.) decrease with α, independently of the functional form of host density-dependence.

The period of the population cycles close to the stability boundary can be calculated using the method described by Murdoch et al. (2002). The coexistence equilibrium of the model is given by (H^*, P^*) and satisfies

$$\frac{r - \mu(H^*)}{a} = P^* = H^* e^{-\alpha\mu(H^*)} \left(1 - e^{-r+\mu(H^*)}\right),$$

with $\mu(H^*) < r$. (5)

The characteristic equation determining the linear stability of this equilibrium is $\lambda^2 + A_1\lambda + A_2 = 0$, where λ is the eigenvalue, and

$$A_1 = \frac{-aH^* e^{-\alpha\mu}}{1 + aP^*/\kappa} + \frac{aP^*}{1 + aP^*/\kappa} - 1 + \mu'H^* \qquad (6)$$

$$A_2 = \left[aP^*\mu'H^*(1-\alpha) + aH^* e^{-\alpha\mu}(1 - \mu'H^*)\right]/(1 + aP^*/\kappa), \quad (7)$$

where $\mu' = d\mu(H^*)/dH^*$. A Hopf bifurcation from a stable host–parasitoid coexistence to population cycles occurs when $A_2 = 1$. The period of the cycles on the stability boundary is then given by

$$\text{period} = \frac{2\pi}{\tan^{-1}\left(\sqrt{\frac{4}{(1+\Omega)^2} - 1}\right)} \quad \text{with } \Omega = -1 - A_1.$$

To ensure that the coexistence equilibrium has undergone no other bifurcation, we need to rule out the occurrence of $+1$ bifurcations and -1 bifurcations. This is equivalent to requiring that the first two Jury conditions are satisfied (i.e. $1 + A_2 > |A_1|$) which is true provided $-3 < \Omega < 1$. The expression for Ω depends on the change in host survival due to competition and parasitism. We can define $\Omega = \Omega_1 + \Omega_2$, where

$$\Omega_1 = \underbrace{-\mu' e^{-\mu}}_{\substack{\text{Change in survival} \\ \text{due to competition}}} H^* e^r f(P^*)$$

$$\Omega_2 = -H^* e^{-\alpha\mu} \underbrace{\frac{df}{dP^*}}_{\substack{\text{Change in survival} \\ \text{due to parasitism}}}.$$

Host survival decreases as hosts increase, so Ω_1 is negative. Host survival decreases as parasitoids increase, so Ω_2 is positive. The period of the consumer–resource cycles increases as Ω increases, and so depends on host survival. We show that for a large class of models, Ω is a decreasing function of α, and thus the period of host–parasitoid cycles decreases with increasing α. To prove this result we first consider the dependency of H^* on α.

3.1.1. Host equilibrium density, H^*, is an increasing function of α

Differentiating Eq. (5) with respect to α and collecting terms gives

$$\frac{dH^*}{d\alpha} \overbrace{\left(\mu' e^{(r-\mu)/\kappa} + (ae^{-\alpha\mu} - \mu'\alpha aH^* e^{-\alpha\mu})(1 - e^{-r+\mu}) - \mu'aH^* e^{-\alpha\mu} e^{-r+\mu}\right)}^{=\Psi}$$

$$= aH^* e^{-\alpha\mu}(1 - e^{-r+\mu})\mu > 0. \tag{8}$$

We show that Ψ is positive. Since $A_2 = 1$ and $\Omega < 1$, it follows that

$$\Psi = \mu' e^{(r-\mu)/\kappa} + \frac{aP^*}{H^*} + \mu'aP^*(1-\alpha) - \mu'aH^* e^{-\alpha\mu}$$

$$= \mu' e^{(r-\mu)/\kappa} + \frac{aP^*}{H^*} + \frac{1 - aH^* e^{-\alpha\mu} + aP^*/\kappa}{H^*}$$

$$> \mu'(e^{(r-\mu)/\kappa} - (1 + aP^*/\kappa)) = 0.$$

Thus, by (8), $dH^*/d\alpha > 0$ and so the value of the host equilibrium increases with α. Therefore, if the parasitoids emerge from the parasitized hosts late in the host life cycle then the equilibrium host density is larger.

3.1.2. Ω is a decreasing function of H^* for all $\kappa \geq 1$

To study the dependency of Ω on H^*, we reformulate Ω in terms of P^* rather than H^*. This turns out to simplify the analysis. We have

$$\Omega = \frac{\frac{aP^*}{1+aP^*/\kappa} - H^*\mu'\left(\frac{1}{f(P^*)} - 1\right)}{\frac{1}{f(P^*)} - 1}.$$

Differentiating Ω with respect to H^* and noting that $\mu' > 0$ for all $\mu(H^*)$ given in Table 1 yields

$$-\frac{\partial\Omega}{\partial H^*}\left(\frac{1}{f(P^*)} - 1\right)^2 = H^*\mu''\left(\frac{1}{f(P^*)} - 1\right)^2 + \mu'\left(\left(\frac{1}{f(P^*)}\right)^2\right.$$

$$\left. - \left(\frac{1}{f(P^*)}\right)\left(\frac{1 + aP^* + 2\frac{aP^*}{\kappa}}{1 + \frac{aP^*}{\kappa}}\right) + \frac{\frac{aP^*}{\kappa}}{1 + \frac{aP^*}{\kappa}}\right). \tag{9}$$

We next show that the term multiplying μ' in (9) is positive. To do this we consider the quadratic

$$Z^2 - Z\frac{1 + aP^* + 2aP^*/\kappa}{1 + aP^*/\kappa} + \frac{aP^*/\kappa}{1 + aP^*/\kappa} = (Z - Z_-)(Z - Z_+),$$

where Z_- and Z_+ are the roots of the quadratic. Descartes' rule of sign tells us that the quadratic has no roots with negative real part; in fact, the quadratic has two positive real roots. The largest root, Z_+, is given by

$$Z_+ = \left[2aP^*/\kappa + 1 + aP^*\right.$$

$$\left. + \sqrt{(aP^* + 1)^2 + 4(aP^*)^2/\kappa}\right] \Big/ (2 + 2aP^*/\kappa).$$

We will show that $1/f(P^*) > Z_+$, and it then follows that the quadratic multiplying μ' in Eq. (9) is positive.

To show that $1/f(P^*) > Z_+$ it is convenient to study $(1/f - Z_+)(1 + aP^*/\kappa)$, which is 0 at $P^* = 0$. By showing that $(1/f - Z_+)(1 + aP^*/\kappa)$ is an increasing function of aP^* for all $aP^* > 0$ and $\kappa \geq 1$, it will follow that $1/f(P^*) - Z_+ > 0$ for all $P^* \geq 0$ and $\kappa \geq 1$.

Differentiating $(1/f - Z_+)(1 + aP^*/\kappa)$ with respect to aP^* and taking $\kappa \geq 1$ gives

$$\frac{\kappa + 1}{\kappa}(1 + aP^*/\kappa)^\kappa$$

$$- \left(2/\kappa + 1 + \frac{aP^* + 1 + 4aP^*/\kappa}{(aP^* + 1)^2 + 4((aP^*)^2/\kappa)^{(1/2)}}\right) \Big/ 2$$

$$> \frac{\kappa + 1}{\kappa}(1 + aP^*) - \left(2/\kappa + 1 + \frac{aP^* + 1 + 4aP^*/\kappa}{aP^* + 1}\right) \Big/ 2$$

$$> aP^* - aP^*/\kappa > 0. \tag{10}$$

So $(1/f - Z_+)(1 + aP^*/\kappa)$ is an increasing function of aP^*, as required. In summary, if $\mu'' \geq 0$ and $\kappa \geq 1$ then all terms on the right hand side of Eq. (9) are positive and $\partial\Omega/\partial H^* < 0$. We have $\mu'' > 0$ for models 2 and 7 in Table 1, and for models 4 and 5 provided $b \geq 1$ (which we now assume; this is the requirement for scramble competition). Hence, for models 2, 4, 5 and 7 the period of population cycles decreases with an increasing α. In Appendix A we extend this result to include the remainder of the models in Table 1.
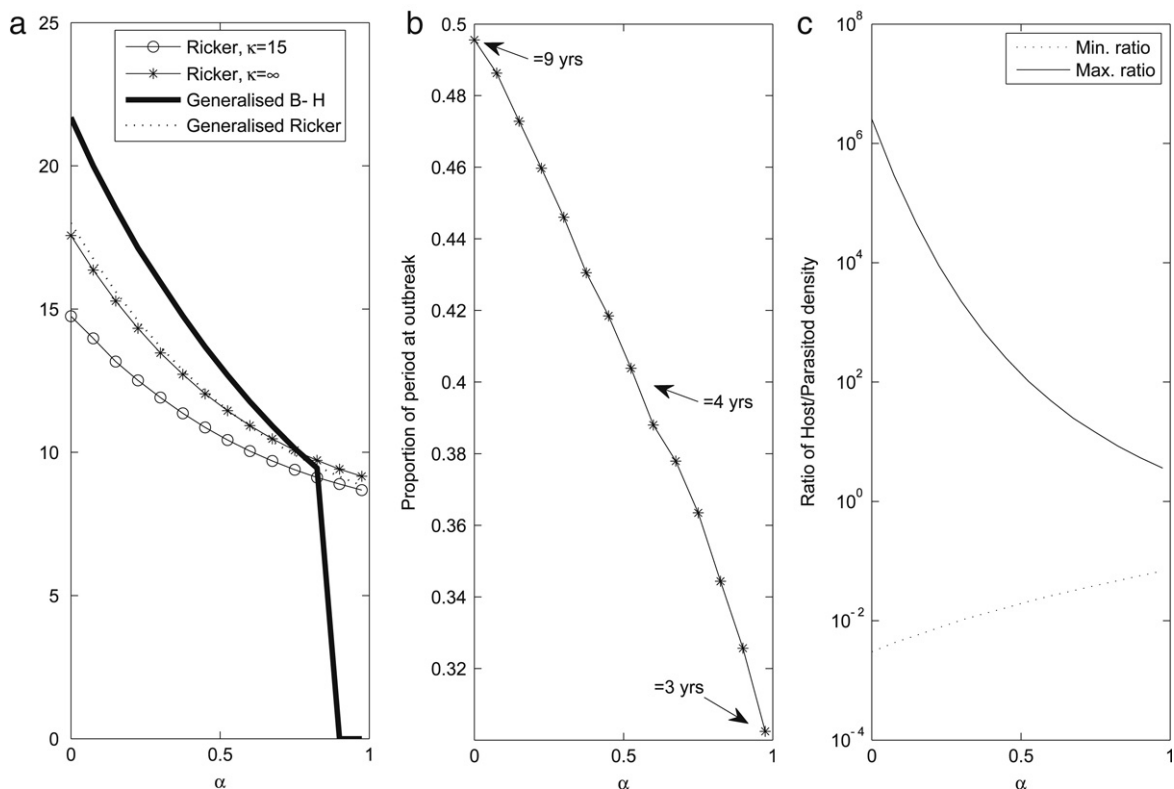
3.2. Numerical study of consumer–resource cycles

The stability analysis does not reveal how α affects the magnitude of changes in period and amplitude of the population cycles. To resolve this, and validate the analysis, we numerically calculate the period and outbreak severity as a function of α (Fig. 2).

The period of the population cycles is estimated to be the average over 10 cycles. The population cycles arise from a Hopf bifurcation, and are therefore aperiodic. The averaging process adjusts for this, producing the smooth curve in Fig. 2a. Outbreak severity is calculated by arbitrarily choosing a cut-off for host density of $0.5K$, then designating densities above this threshold as outbreak densities and below as non-outbreak. The proportion of one period which the host spends above this threshold is calculated and averaged over 10 cycles.

The designation of $0.5K$ as the outbreak threshold is clearly arbitrary. However, for completeness, we calculated the outbreak length using a range of thresholds. The result was slight variation in outbreak lengths but no variation in the overall trends, providing evidence that this is a reasonable measure for the trends in outbreak severity.

The numerical results in Fig. 2 agree with the analytical predictions. Parasitoids that emerge late in the host development exhibit population cycles with a shortened period compared to parasitoids emerging from early host stages. Thus, discrete-time host–parasitoid models that assume functionally dead parasitized hosts ($\alpha = 0$) potentially overestimate the period of population cycles. These results hold for $\kappa \geq 1$; however, for small κ the

Fig. 2. (a) Numerical estimation of the period of the host–parasitoid population cycles as a function of α. As α increases, the period of the oscillations decreases. A cubic least squares fit through the simulation points illustrates this decreasing trend. (b) Outbreak severity plotted as a function of α. Over one period, outbreak severity is the proportion of that period for which host density is above an arbitrary threshold of $0.5K$. Above this threshold is classified as outbreak and below as non-outbreak. The outbreak measure has been averaged over 10 cycle lengths. (c) The maximum and minimum values of the ratio host/parasitoid density reached during one oscillation, plotted against α. Parameter values used to generate these profiles are as follows: $r = 0.9$, $\alpha = 0$, $aK = 8$, $\kappa = \infty$ (random searching), where functions μ and f are as in Fig. 1. The bold and dotted lines in plot (a) are the results of the generalized Beverton–Holt $\mu(H_t) = \ln(1 + (e^r - 1)^b(H_t/K)^b)$, and the generalized Ricker $\mu(H_t) = \ln(r(H_t/K)^b)$, respectively, with $b = 0.8$. To illustrate the effect of κ, the open circles illustrate the case of $\kappa = 15$. Simulations were run for 7000 iterations to ensure the absence of transients, then the period and outbreak duration were calculated.

period of the population cycles is reduced and the effects of α are less pronounced. So clumped parasitism can lessen the effects of parasitoid phenology.

Figs. 2 and 3 show that the duration of the host outbreak decreases with α. Fig. 2c depicts the maximum and minimum values of the ratio host/parasitoid as a function of α and indicates that fluctuations in host and parasitoid numbers are greater for small α. Parasitoids that emerge early (small α) experience low mortality from host competition, but go on to suffer from the effects of their own efficiency. Early-emerging parasitoids increase rapidly in response to host numbers, which leads to a collapse in the host population. Host collapse is followed by a severe parasitoid decline, allowing the host numbers to recover and remain unchecked while parasitoids re-establish following their near extinction. This gives rise to long host outbreaks. In contrast, late-emerging parasitoids experience high mortality from host competition, thus parasitoid numbers increase more slowly in response to high host numbers. Late-emerging parasitoids are regulated by the host, preventing the boom-bust dynamics of more efficient early-emerging parasitoid. Consequently, late-emerging parasitoids have a much tighter control of the hosts, reducing the occurrence of host outbreaks.
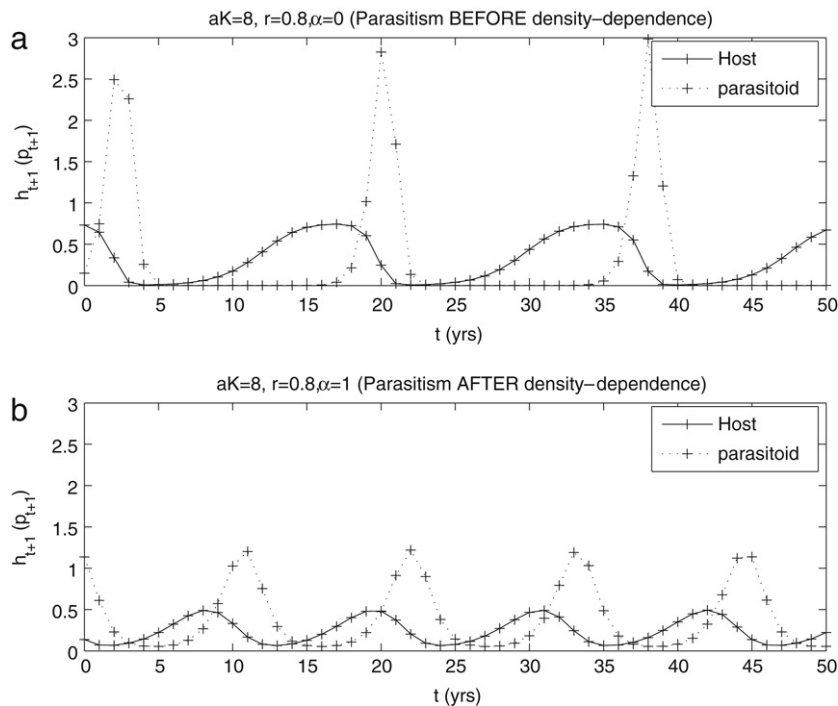
3.3. From scramble to contest competition

The generalized Beverton–Holt and generalized Ricker models of density-dependence (entries 4 and 5 of Table 1) have been found by Getz (1996) and Bellows (1981) to be good descriptors of host competition data. The additional parameter b, for $b > 1$, describes the strength of density-dependent effects on populations

below the model carrying capacity. The parameter b can also indicate where on the competition spectrum (between contest and scramble competition) the model lies, with a large b corresponding to scramble competition. The analysis in Section 3.1 only holds for $b \geq 1$ and fails to cover the case of strong contest competition. Fig. 2 illustrates the results of numerically exploring the case $b < 1$. The results of Section 3.1 continue to hold and late-emerging parasitoids lead to shorter population cycles. Large values of α cease to give rise to host–parasitoid cycles when $b \ll 1$. This is not unexpected, as contest competition is generally recognized as a stabilizing factor. However, we find that contest competition gives population cycles with an increased period and the effect of α is more pronounced. Thus phenology has a greater impact on host–parasitoid dynamics when there is contest competition.

The general trends concerning the characteristics of host–parasitoid population cycles are unaffected by the type of competition between the parasitized and unparasitized hosts. The regulation of the parasitoid by the host stabilizes the dynamics. So although the average host density increases with α, the extremes in host numbers are reduced, allowing the late-emerging parasitoid to more tightly regulate the host. In the next section we fit the model to data from the forest tent caterpillar system and test our theoretical results.

4. Application to the forest tent caterpillar system

The forest tent caterpillar is a mass defoliator of trembling aspen (*Populus tremuloides*) forest stands in North America. The caterpillar periodically reaches outbreak densities, which can
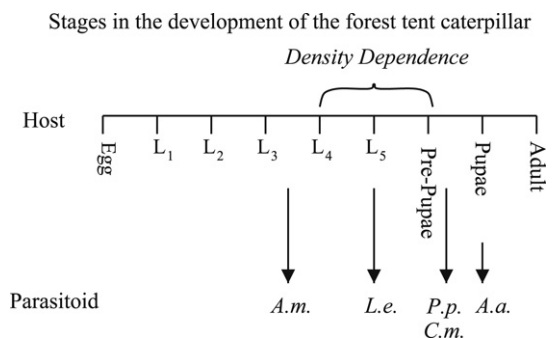
Fig. 3. (a) Numerical time series generated from Eq. (1) with μ and f as in Fig. 1 and $\alpha = 0$. The solid line indicates the host and the dashed line the parasitoid density. The parasitoids reach high densities which then crash alongside the host population. Recovery of the parasitoid population is delayed and hosts are allowed to maintain outbreak densities for a number of consecutive years. (b) Numerical time series generated for $\alpha = 1$. The maximum parasitoid density reached is lower and host outbreaks are shorter. The model was run for 1000 generations and the final 50 were plotted to avoid transients. The carrying capacity of the host population was scaled to 1. The other model parameters used are $aK = 8, r = 0.9$ and $\kappa = \infty$.

be maintained for up to six years, although on average last for 2–3 years (Sippell, 1962). Typically outbreaks occur every 10–12 years (Hodson, 1941; Cooke and Lorenzetti, 2006). During a recent outbreak in Ontario in 1991, 1.9 million hectares of forest were defoliated (Anon, 1991). These attacks seldom result in tree death, but growth loss and dieback are common. The exact cause of this periodic behavior is not known, but connections have been made to both climate patterns (Roland et al., 1998) and the tight linkage with fly and wasp parasitism (Parry, 1994, 1995; Roland et al., 1997).

Both the forest tent caterpillar and most of the fly and wasp species that parasitise it have univoltine life cycles with non-overlapping generations. This makes the system an ideal candidate for our discrete-time model. The forest tent caterpillar has five larval stages. During the first three, larvae are gregarious, staying on the tree where hatching occurred; foliage consumption is low, of the order of one leaf per larva. In the fourth and fifth larval stages the caterpillars are solitary and more mobile, with feeding increasing significantly. At high larval densities this induces strong competition for resources and potential larval mortality, as evidenced by the experiments discussed in Appendix B.1. Some species of specialist parasitoid oviposit on host pupae, while others attack larval stages (see Fig. 4). Although one parasitoid species generally dominates parasitism at any given field site, this can differ among sites.

Appendix B describes the experimental data, model fitting and parameter estimation. Table 1 and Fig. 5 summarize the results. Ricker density-dependence (entry 2, Table 1) provides the most parsimonious model of host competition. The Poisson model, $f(P_t) = \exp(-aP_t)$, gives the best fit to the parasitism data. Lastly, field experiments (Appendix B.1) allow us to estimate α for each parasitoid species (Fig. 6).

The parameterised host–parasitoid model exhibits periodic oscillations in H_t and P_t for all values of α, consistent with the periodic outbreaks found in forest tent caterpillar time series. To
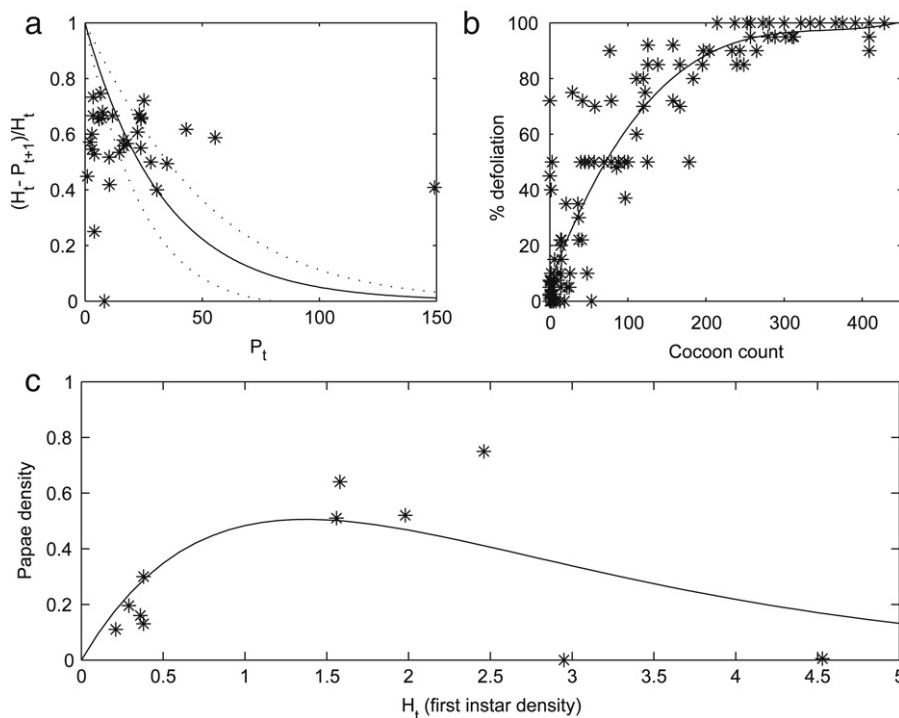

Fig. 4. Schematic of the developmental stages of the forest tent caterpillar. L_i refers to the ith larval instar. Forest tent caterpillars carry out a majority of their food consumption during the life stages indicated by density-dependence. The arrows indicate on average which stage in the life cycle a parasitoid would emerge from the host. *A.m., Aleiodes malacosomatus*, is a wasp species. *L.e., Leschenaultia exul*, and *P.p., Patelloa pachypyga*, are more common parasitoids of the fly family Tachinidae. *A.a, Arachnidomyia (=Sarcophaga) aldrichi* (Sarcophagidae), is an aggressive pupal parasitoid, as is *C.m., Carcelia malacosomae* (Tachinidae).
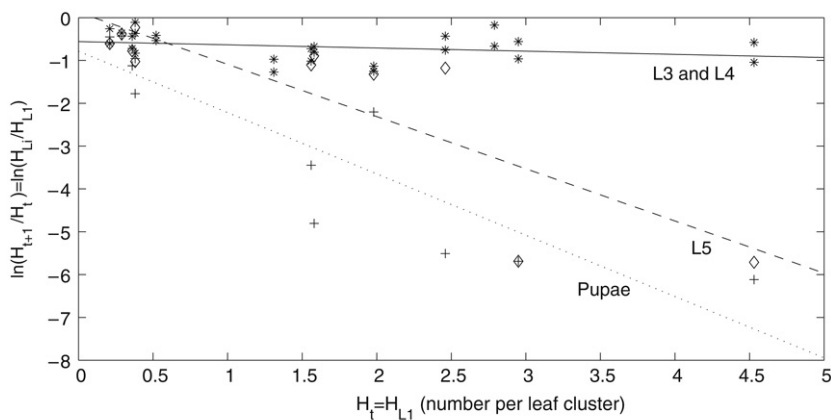
allow for the fact that natural systems are composed of more than one parasitoid species, we take $\alpha \in [0, 1]$ as a free parameter and validate the model against an independent time series from Hodson (1941).

4.1. Validation of the model

Using the methods described in Appendix B.2.2 we examine the correlation between Hodson's data and the time series generated by Eqs. (1). Fig. 7a gives the binary correlation coefficient as a function of α. Correlation with the Western Canada data set is maximized when $\alpha \approx 0.35$, with 78% correlation. The correlation is considerably higher than when $\alpha = 0$ or $\alpha = 1$, so the data lends some support to our argument that parasitoid phenology may be an important descriptor of host–parasitoid interactions.

Fig. 5. (a) Fit of $f(P_t) = e^{-aP_t}$ to the 1994 parasitism data of Appendix B.2. The line indicates the best fit and the two dotted lines are the 95% confidence interval. (b) Forest tent caterpillar defoliation data for 1994 (see Appendix B.2.1) used to estimate host carrying capacity, K. (c) Fit of $\mu(H_t) = -cH_t$ to the host survival data discussed in Appendix B.1.
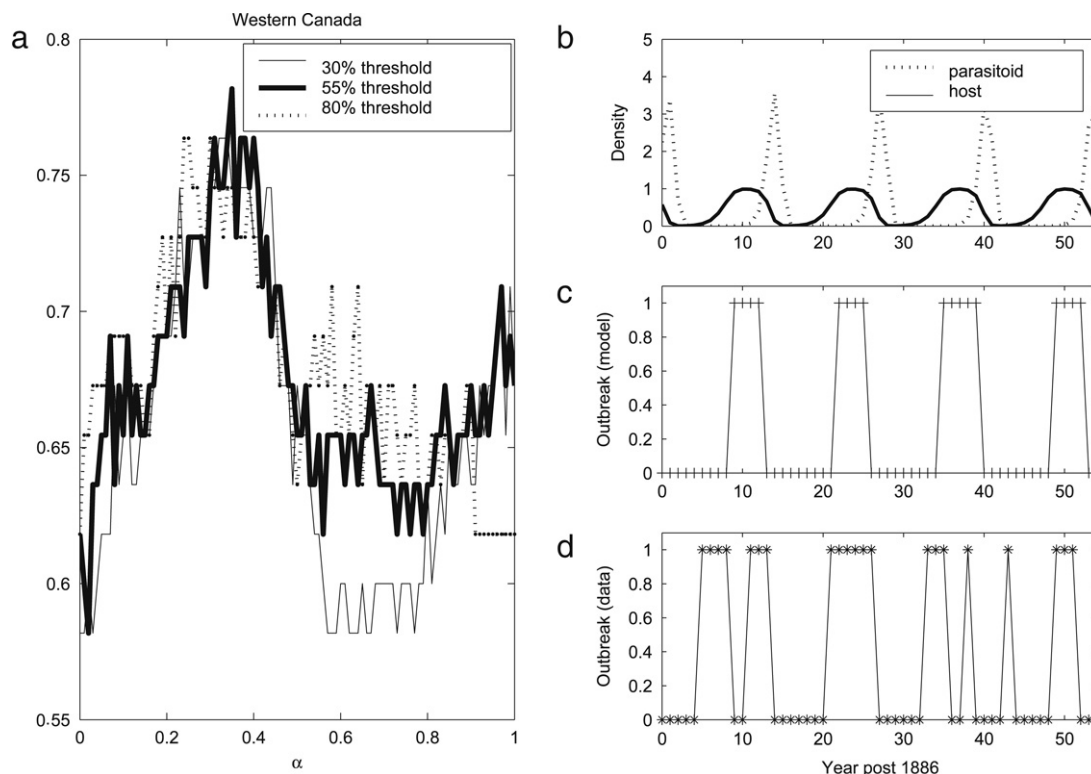

Parasitoid	Emergence time	Average emergence instar in Alberta (Parry (1994))	α
Aleiodes malacosomatus	3rd / 4th instar	3.5	0.0
Leschenaultia exul	5th instar	6.1	0.865
Carcelia malacosomae	Late 5th instar / pupae	6.87	0.905
Patelloa pachypyga	Pupae	6.96	0.994
Arachnidomyia aldrichi	Pupae	7	1.0

Fig. 6. Graphs of the log of the ratio of host density at instar L_i to host density at instar L_1 plotted against density at L_1. A linear regression through the data points for each instar, provides a slope which estimates α. (Data for survival to the 3rd and 4th instar is denoted by $*$, to the 5th instar by $\diamond$, and to pupation by $+$). Equations of the regression lines are as follows: for instar 3 and 4, $\ln(H_{t+1}/H_t) = -0.579 - 0.068H_t$; for instar 5, $\ln(H_{t+1}/H_t) = 0.163 - 1.231H_t$; for pupae, $\ln(H_{t+1}/H_t) = -0.958 - 1.373H_t$. We notice that the gradient of the regression lines decreases as larval stage increases. This is consistent with the fact that larvae do most of their eating in the later stages of development. Using the average instar at which emergence of each parasitoid species occurs we have calculated α for FTC populations in Alberta. When estimating α, 1–5 refers to larval instars 1–5 respectively; 6 = pre-pupae, and 7 = pupal stage.

We also calculated the binary correlation coefficients to data from other regions of North America and consistently found that the correlation between the model and data is highest (75%–95%) for intermediate values of α. The remaining model parameters used in these fits are taken from the Alberta data, so we must be careful not to conclude too much from fitting this to other North

Fig. 7. (a) Binary correlation coefficient ρ, as a function of α. The parameter ρ describes the proportion of matching between the time series data and the model. The lines correspond to different thresholds for categorizing an outbreak in the model. (b) A time series solution of the model for host and parasitoid density. (c) The model time series plotted as presence/absence of an outbreak using a threshold of 80% of host carrying capacity, with $\alpha = 0.35$, the value of α that maximizes the correlation between model and data. (d) Time series data from Hodson (1941) used to validate the model. The remaining parameter values used to generate these profiles are as follows: $r = 0.96$, $aK = 8$ and $\kappa = \infty$.

American regions. However, the high correlations suggest that the model framework provides a reasonable description of forest tent caterpillar dynamics.

4.2. Interpretation of model results

In a field setting the late-emerging parasitoid *A. aldrichi* drops out of the system at low host densities, while the early-emerging *A. malacosomatus* continues to parasitize at low host densities (Cooke, 2001; Parry, 1994). Although we consider only a single-parasitoid model, Fig. 3 shows that late-emerging parasitoids do not deplete the host population as severely as early-emerging parasitoids. The model suggests that early-emerging parasitoids can persist at very low host densities, which is consistent with experimental observations. In the two years following a general population decline, Hodson (1941) found one caterpillar after repeated searching in 15 study plots and the surrounding areas. Similar observations of extremely low population levels have been reported elsewhere.

Sippell (1957) studied the prolonged caterpillar outbreaks in Ontario, recording the early-emerging parasitoid *A. malacosomatus* as being more abundant in Ontario than in other locations where outbreaks were shorter. This is consistent with our model prediction that early-emerging parasitoids are associated with longer population outbreaks.

4.3. Stochasticity

To test the robustness of our model to environmental stochasticity, we multiplied the right-hand side of (1a) by a log-normally distributed random variable ϵ_t with mean 1 and standard deviation 0.3. Using the forest tent caterpillar parameters (with $\alpha = 0.35$) as a reference point, we found that introducing stochasticity had little

effect on the model output and in fact improved the fit of the model time series to the data (Table 2). In contrast, when we included stochasticity for the case $\alpha = 0$ we found that the average period of the host population cycles increased by 50%. While Hodson's data gave an average period of 11 years between outbreaks, the model ($\alpha = 0$) gave 18 years. The other model descriptors were equally poor and failed to fall within two standard deviations of the data.

From Fig. 1a, when $\alpha = 0$ the parameter set lies close to a stability boundary, and stochasticity allows the model to enter the region of chaotic dynamics. Dwyer et al. (2004) found a similar phenomenon in their study of gypsy moth dynamics. When $\alpha > 0$, parameters remain away from stability boundaries (*cf.* Fig. 1c) and the host–parasitoid dynamics do not jump between attractors. In a host–pathogen-generalist predator model of gypsy moth outbreaks, Dwyer et al. (2004) found that a significantly better explanation of the data could be achieved by adopting a combined effect model, whereby the dynamics jumped between multiple attractors via 'environmental stochasticity'. The more predictable nature of forest tent caterpillar outbreaks, and the improved fit by the stochastic model for $\alpha \neq 0$, suggest that jumping between multiple attractors may not be occurring in the forest tent caterpillar system. An important feature of the forest tent caterpillar system is the regional variation in cycle length, for example, between the provinces of Ontario and Alberta in Canada (Cooke and Lorenzetti, 2006). The variation coincides with differences in the composition of the parasitoid communities and these differences may be an important factor in determining outbreak duration.

4.4. Extension to multiple parasitoid species

Hosts are often exposed to numerous species of specialist parasitoids, as observed in the forest tent caterpillar system. It is

Table 2
Descriptors of Hodson's data are calculated for 9 regions in North America.

Location	Mean period (standard deviation)	Mean outbreak duration (standard deviation)	Mean non-outbreak duration (standard deviation)
Western Canada	7.33 (2.94)	3.00 (1.90)	4.33 (2.07)
Central Canada[a]	11.25 (7.89)	3.40 (3.36)	9.00 (8.91)
Eastern Canada	11.50 (1.73)	3.75 (1.26)	7.75 (1.26)
Washington	9.20 (2.17)	3.20 (2.17)	6.00 (4.00)
Maine	12.00 (1.41)	5.25 (1.50)	6.75 (0.96)
New Hampshire[a]	15.33 (6.05)	4.25 (1.26)	11.67 (6.03)
Vermont[a]	19.00 (4.24)	5.00 (1.41)	14.00 (5.66)
Massachusetts	8.00 (4.52)	2.33 (1.37)	5.67 (3.33)
Minnesota	8.40 (3.36)	2.83 (2.14)	6.20 (3.63)
Model (Eqs. (1)), $\alpha = 0$	18 **[26.85 (24.75)]**	9.99 **[25.82 (24.75)]**	8.01 **[1.03]**
Model (Eqs. (1)), $\alpha = 0.35$	13.05 **[9.57 (3.22)]**	5.3 **[5.05 (2.25)]**	7.75 **[4.52]**

[a] Needs to be viewed with caution. The large standard deviations for the Central Canadian data are due to only sporadic one-year outbreaks prior to the 1920s. The Vermont data contains only two full outbreaks, thus the absence of an outbreak in the 1920s has a large effect on the mean period; similarly for New Hampshire. The last two entries in the table give the results predicted from Eqs. (1) with $\alpha = 0$ and $\alpha = 0.35$; all other parameters and choices for f and μ are as in Fig. 2. Eqs. (1) with $\alpha = 0$ poorly describe the data, overestimating outbreak duration and frequency, while Eqs. (1) with $\alpha = 0.35$ is more parsimonious. The numbers in bold refer to the results of the stochastic model with forcing term ϵ_t.

therefore important to know if our findings extend to multi-parasitoid systems. A simple model extension to the multi-parasitoid system is given by

$$H_{t+1} = H_t e^r e^{-\mu(H_t)} f(P_t; a_P) f(Q_t; a_Q) \tag{11a}$$

$$\boxed{\text{Late}}\; P_{t+1} = H_t e^{-\alpha_P \mu(H_t)} \left[\overbrace{\frac{\text{Fraction of hosts}}{(1 - f(P_t; a_P)) f(Q_t; a_Q)}}^{\substack{\text{Fraction of hosts} \\ \text{parasitized by } P, \text{ NOT } Q}} \right.$$

$$\left. + \overbrace{\phi(1 - f(P_t; a_P))(1 - f(Q_t; a_Q))}^{\substack{\text{Fraction of hosts} \\ \text{parasitized by } P \text{ and } Q, P \text{ WINS}}} \right] \tag{11b}$$

$$\boxed{\text{Early}}\; Q_{t+1} = H_t e^{-\alpha_Q \mu(H_t)} \left[\overbrace{(1 - f(Q_t; a_Q)) f(P_t; a_P)}^{\substack{\text{Fraction of hosts} \\ \text{parasitized by } Q, \text{ NOT } P}} \right.$$

$$\left. + \overbrace{(1 - \phi)(1 - f(P_t; a_P))(1 - f(Q_t; a_Q))}^{\substack{\text{Fraction of hosts} \\ \text{parasitized by } P \text{ and } Q, Q \text{ WINS}}} \right], \tag{11c}$$

which builds on the model by Hogarth (1984). The function $f(P_t; a_P) = (1 - a_p P_t / \kappa)^{-\kappa}$ is the probability of the host escaping parasitism by P, $f(Q_t; a_Q)$ is the corresponding function for parasitism by Q. The subscripts on the parameters refer to parasitoids P and Q. The model allows for the possibility of multi-parasitism. The final term in each parasitoid equation denotes the probability that both P and Q parasitize the host and ϕ is the probability that P successfully outcompetes Q and the multi-parasitized host produces parasitoids of type P.

The model captures a broad spectrum of multi-parasitoid interactions, however as mentioned in the introduction the timing of parasitoid attack becomes relevant when more than one parasitoid species is present. In this preliminary extension to the multi-parasitism case we assume that the two parasitoid species attack the same host stage and only their emergence time differs. We define P as the late-emerger ($\alpha_P = 1$) and Q as the early-emerger ($\alpha_Q = 0$) and investigate how the timing of parasitoid emergence effects host–parasitoid population cycles. In the simple case where multi-parasitized hosts always produce parasitoids of type Q ($\phi = 0$) we 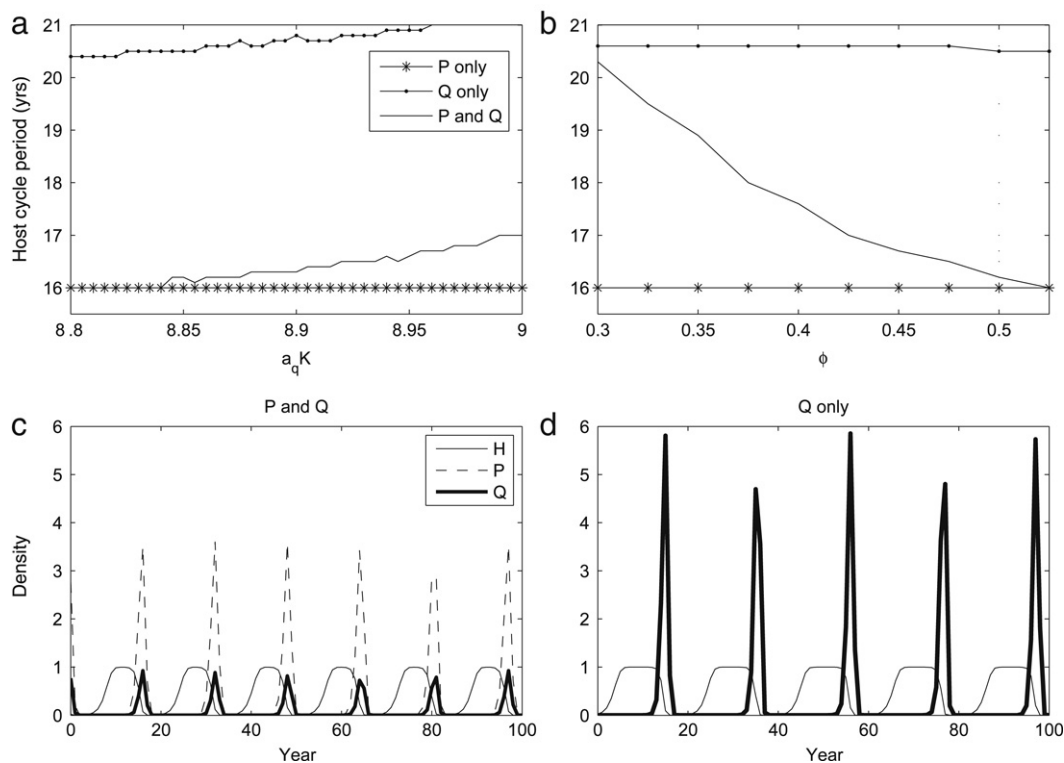can prove that the coexistence of two parasitoid species, one emerging earlier than the other, cannot occur when the searching efficiency of the late parasitoid is less than or equal to that of the early parasitoid (see Appendix C). This finding is consistent with the fixed-delay model of Briggs et al. (1993) which showed that coexistence was not possible when two parasitoid species attacked different developmental stages.

In the case where $\phi \neq 0$ coexistence is possible. Numerical results have lead us to conjecture that the late-emerging parasitoid drives the period of oscillations in a multi-species system (Fig. 8). The significance of this observation is that most discrete-time host–parasitoid models implicitly study early-emerging parasitoids by omitting competition between parasitized and unparasitized hosts. We suggest that late-emerging parasitoids may be more important in driving cyclic dynamics in natural systems. In the forest tent caterpillar example it is generally thought that *A. aldrichi* and *P. patelloa* drive the caterpillar dynamics, and these are indeed the late-emerging parasitoid species (Cooke, 2001).

In Fig. 8(a) and (b) we plot the period of the host cycles as a function of $a_Q K$ and ϕ respectively. We find that increasing the searching efficiency of parasitoid Q (early-emerger) has very little affect on the period of host cycles. The period is close to that found when only parasitod P is present. Increasing ϕ, allowing the late-emerging parasitoid to be most successful during multiparasitism, decreased the period of the host cycles. When $\phi \approx 0.5$ the host period is the same as when only parasitoid P is present. Fig. 8(c) and (d) illustrate the temporal evolution of the host–parasitoid cycles, with and without the late-emerging parasitoid respectively. The dynamics of parasitoid Q are constrained by the presence of P and the late-emerging parasitoid drives the host–parasitoid dynamics.

5. Discussion

With a few notable exceptions (Wang and Gutierrez, 1980; May et al., 1981), discrete-time host–parasitoid models have not addressed the role of parasitoid phenology in determining host–parasitoid dynamics. The general framework presented in this paper allows parasitoid emergence phenology to be described relative to events in the host's yearly life cycle. Explicitly, we describe competition between parasitized and unparasitized hosts that occurs when parasitoid development overlaps with the period of host density-dependent competition. We examined the effect of parasitoid emergence time under a range of competition models and found that our qualitative conclusions were independent of the precise type of competition experienced by the parasitized and unparasitized hosts.

Fig. 8. (a) and (b) The period of the host cycles is shown as a function of $a_Q K$ and ϕ respectively. The solid line indicates the period when both parasitoids are present. The starred line corresponds to P only and the spotted line is Q only. (c) and (d) Host–parasitoid cycles are plotted as a function of time. The parameters for all plots are given by: $r = 0.96, a_P K = 14.8, a_Q K = 8.9, \phi = 0.5, \alpha_P = 1, \alpha_Q = 0$ and $\kappa = \infty$ except in the case where a parameter was varied. The mortality function is given by $\mu(H_t) = rH_t/K$. In (a) and (b) we see that the period of host cycles in the full $H–P–Q$ system is always below that of the $H–Q$ only system. The late-emerging parasitoid drives the population cycles. Increasing the searching efficiency of parasitoid Q leads to only a slight increase in host period above that of the $H–P$ only system. Only when Q is significantly more successful in multiparasitizing the host is the host period closer to that of the $H–Q$ system.

Analysis of the equilibrium dynamics of the model showed that late-emerging parasitoids (large α) are susceptible to extinction when host growth rates are high, while early-emerging parasitoids (small α) can coexist with the host. These seemingly paradoxical results arise from the nonlinear host population dynamics which exhibit overcompensation. The coefficient α can be considered a scaling factor that determines the strength of the nonlinear overcompensation experienced vicariously by the parasitoid when it resides in the host. Those parasitoids that emerge early escape the strongest effects of overcompensation, while late-emerging parasitoids experience the full overcompensation. Overcompensation is not simply a model artefact. It is typical of host–parasitoid models, and the Ricker model, determined to be the most parsimonious for our forest tent caterpillar data (Table 1), exhibits this feature also. When the parasitoid is late-emerging, it may still be able to control the host population, providing the intrinsic growth rate for the host r is sufficiently small.

Parasitoids are commonly used as biological control agents for pest host species. In this case correctly predicting persistence of the parasitoid is essential, so knowledge of the timing of parasitism and the host growth rate become important when selecting a suitable biological control agent. We infer that habitats that promote a high host growth rate for hosts may only be able to support early-emerging parasitoids. Fragmented habitats, often associated with low host growth, may be better suited to biological control from late-emerging parasitoids.

The main focus of this work has been the study of the host–parasitoid population cycles. The period and the amplitude of these cycles increase with decreasing α, independent of our choice of competition. The model shows that late-emerging parasitoids have a stabilizing effect on host–parasitoid dynamics, by reducing the amplitude of population cycles. Parasitoids that emerge early

from the host induce long host outbreaks. This is particularly significant for our biological example, the forest tent caterpillar. Prolonged outbreaks of the forest tent caterpillar can lead to long-term tree damage, which can have an significant socio-economic impact. When minimizing the outbreak duration is the objective of biological control, late-emerging parasitoids would be the preferred choice of agent.

The modeling formulation presented in this paper is general so that the type of competition between hosts (parasitized or unparasitized) can vary during the hosts life-cycle. However, the results in this paper are confined to studying the case where the type of competition remained unchanged during the season, or more generally α remained independent of H_t. While these results apply to many host–parasitoid systems there is evidence to suggest that the type of competition can change during the host life-cycle in some systems. In particular, Lane and Mills (2003) found that in the *Ephestia keuhniella–Venturia canescens* laboratory system, the presence of parasitoids resulted in the host competition changing from scramble competition to contest competition. This offers an interesting direction for future work. Within season changes in competition type can easily be incorporated into the model and may have a significant influence on the population dynamics between parasitized and unparasitized hosts. Moreover, it is no longer just the parasitoid emergence time that needs to be considered, but also the length of time a parasitoid spends in the host.

Another important factor that could influence the role of parasitoid emergence on the population dynamics is the presence of more than one natural enemy. Specifically, more that one parasitoid. Preliminary work in Section 4.4 suggests that the later-emerging parasitoid governs the period of host population cycles in a multi-parasitoid system, although clearly this needs further

exploration as we have restricted ourselves to only considering parasitoids which attack their hosts at the same time. The preliminary results do emphasize the importance of considering parasitoid timing in discrete-time models. Age-structured models have already indicated the importance parasitoid timing for non-diapausing insects (Briggs et al., 1993, 2000), we now find that parasitoid timing also impacts on diapausing insects.

Our main result from this paper has shown that host regulation of the parasitoid has important implications for the host–parasitoid dynamics. Early-emerging parasitoids induce more severe host outbreaks, resulting from a less controlled response to host numbers. The results from this work may have an application for other biological systems. For example, Bonsall et al. (1999) studied phenology in a hybrid discrete-time host–pathogen model in which host density-dependence acted during the window of susceptibility to a pathogen. They found that the likelihood of population cycles depended on the strength of host density-dependence. We have similar findings, suggesting that the behavior shown in this paper may not be limited to only host–parasitoid systems, but might also apply to other systems in which the mortality of an infected host is delayed. Our work may have further implications for host populations whose larval development is coupled to temperature or other developmental cues: faster-developing hosts could release parasitized hosts from competition more quickly, which could in turn promote host outbreaks. Many aspects of insect life-cycles, such as phenology are coupled to environmental cues so an understanding of how parasitoid-phenology effects host–parasitoid population dynamics can offer insights into how systems may respond to environmental changes.

Acknowledgments

Appendix A. Trends in cycle period for the case $\mu'' + (\mu')^2 \geq 0$

All the models of density-dependence presented in Table 1 satisfy $\mu'' + (\mu')^2 \geq 0$ when $b \geq 1$. We extend the results of Section 3.1 to this larger class of mortality functions in the limiting case $\kappa \to \infty$; then $f(P_t) = e^{-aP_t}$. We first reformulate $A_2 = 1$ in terms of P^*, giving

$$aP^* \left(e^{aP^*} - H^* \left(\alpha \left(e^{aP^*} - 1 \right) + 1 \right) \mu' \right) = e^{aP^*} - 1.$$

The left hand side decreases with α. Let $\epsilon \geq 0$; then for $\epsilon \leq \alpha \leq 1$, we have

$$\mu' H^* < \frac{aP^* e^{aP^*} - e^{aP^*} + 1}{aP^*(e^{aP^*}\epsilon + (1-\epsilon))}.$$

Using this inequality and $\mu'' + (\mu')^2 \geq 0$ with Eq. (9) yields

$$-\frac{\partial \Omega}{\partial H^*} \frac{(e^{aP^*} - 1)^2}{\mu'} \geq \frac{s_\epsilon(P^*)}{aP^*(e^{aP^*}\epsilon + 1 - \epsilon)}, \tag{A.1}$$

where

$$s_\epsilon(P^*) = (e^{aP^*} + 1 - aP^*)e^{aP^*} aP^*(e^{aP^*}\epsilon + 1 - \epsilon)$$
$$- (e^{aP^*} - 1)^2 (aP^* e^{aP^*} - e^{aP^*} + 1).$$

It can be shown that for $aP^* < 0.75$, we have $s_0(P^*) \geq s_\epsilon(P^*) > 0$ for all ϵ. As $aP^* = r - \mu < r$, we can conclude from Eq. (A.1) that if $r < 0.75$ then $\partial \Omega / \partial H^* < 0$.

An alternative condition for arbitrary r to give $\partial \Omega / \partial H^* < 0$ requires that $\alpha > \epsilon = 0.67$. In other words, for an arbitrary choice of r we need $s_\epsilon(P^*) > 0$ for all $\alpha > 0.67$. This is found by using the condition that $\Omega > -3$, which gives

$$\Omega + 3$$
$$= \frac{(\alpha(e^{aP^*} - 1) + 1)(aP^* + 3(e^{aP^*} - 1)) + (e^{aP^*} - 1 - aP^* e^{aP^*})(e^{aP^*} - 1)}{(e^{aP^*} - 1)(\alpha(e^{aP^*} - 1) + 1)}$$
$$> 0. \tag{A.2}$$

Let $q(P^*)$ denote the numerator of the above expression. Then q is positive for $0 \leq P^* < P_\alpha$, where P_α is the root of q. These values of P^* are precisely those parasitoid fixed points that satisfy the conditions for limit cycle existence. Thus, it suffices to show that $\partial \Omega / \partial H^* < 0$ for these values of P^*. To show this is true we bound $\mu' H^*$ using the constraint $\Omega > -3$, and apply this bound to (9). This gives

$$-\frac{\partial \Omega}{\partial H^*} \frac{(e^{aP^*} - 1)^2}{\mu'} \geq u(P^*), \tag{A.3}$$

where $u(P^*) = (e^{aP^*} - 1 - aP^*)e^{aP^*} - (3 + aP^*)(e^{aP^*} - 1)$. But $u(P^*) > 0$ for all $P^* > 2$, so for $2 < P^* < P_\alpha$ we have $\partial \Omega / \partial H^* < 0$.

It now remains to show that $\partial \Omega / \partial H^* < 0$ for $0 < P^* < 2$. By Eq. (A.1) this is true for $\alpha > \epsilon = 0.67$. We conclude that for arbitrary r the period of population cycles decreases with α, for all $\alpha > 0.67$. For the forest tent caterpillar data, $r = 0.9$, the condition on α given above becomes less restrictive, and for all $\alpha \geq 0.25$ we have $s_\epsilon(P) > 0$; hence by Eq. (A.1), $\partial \Omega / \partial H^* < 0$.

Appendix B. Forest tent caterpillar data and the estimation of parameters

B.1. Experimental protocol for the estimation of α

The parameter α was determined by estimating the density-dependent mortality of each larval instar of the host caterpillar in the absence of parasitism by any species.

B.1.1. Experimental treatments

Fifteen trees were selected within a 0.5 ha area of continuous aspen forest in the Cooking Lake Blackfoot Wildlife Recreation Area; approximately 35 km east of the city of Edmonton, Alberta, Canada. At this site, there had been an outbreak of forest tent caterpillars that had collapsed in 1996, six years prior to our experiment. Forest tent caterpillar egg masses from an outbreak population near Rocky Mtn. House, Alberta, approximately 200 km southwest of the study site, were attached to the trees. The number of eggs in an egg mass varied, but averaged about 200. Trees received one of three treatments in the first week of May before the normal time of egg hatch (about May 10): 1 egg mass per tree, 5 egg masses per tree, and 10 egg masses per tree. Because the number of eggs per mass varied, egg masses were re-collected at the end of the experiment so that we could count the exact number of caterpillars that successfully hatched on each tree. The number of leaf buds were also counted on each tree so that an estimate of hatched caterpillars per leaf cluster could be calculated for each tree. As a result, instead of three density treatments, we ended up with a range of caterpillar densities among the 15 trees ranging from 0.20 to 4.6 first instar larvae per leaf cluster.

Twelve of the 15 trees were enclosed in a fine-mesh cage that excluded all parasitoids. Cages were approximately 3 m tall and 1.5 m in diameter, were gathered at the trunk, and enclosed the entire canopy of the tree. Cages had a zipper running their full

height so that all parts of the canopy could be easily accessed and sampled from a step ladder. One of the cages was not completely sealed and caterpillars escaped; this tree was excluded from the study. The remaining 3 trees were uncaged to assess the effect of the mesh cage on the host behavior until the fourth instar when the larvae become more mobile.

The number of caterpillars surviving in each cage was initially counted twice per week, but when caterpillars had reached 5th instar they were counted every second day. Once all caterpillars had either died or successfully pupated in a cage, the pupae were counted, collected and weighed to the nearest mg.

B.1.2. Host density-dependence model selection and parameter estimation

Seven models of host density-dependence, (see Table 1), were fitted to the experimental data using maximum likelihood fitting assuming normally distributed error. The seven models were then compared using corrected Akaike information criteria (AICc) (Akaike, 1974).

Density-dependence is strongest in the later life stages. Density-dependence in the early stages, instars 3 and 4, is not significant, consistent with behavioral observations for these instars. Survival to the end of instar 5 was used to fit the models for $\exp(-\mu(H_t))$. The results are summarized in Table 1 and illustrated in Fig. 5. Entry 2, Ricker density-dependence, has the lowest AICc and is the most parsimonious description of forest tent caterpillar density-dependence.

Using the approach described in Section 2.1, we estimate α by fitting a Ricker density-dependence model to the instar survival data described in Appendix B.1. Using the average parasitoid emergence times for five parasitoid species taken from Parry (1994), we calculate α for each of the major species of parasitoid that attack the forest tent caterpillar. Our estimates of α are likely to be overestimates of density-dependent mortality of parasitized hosts, because at very high densities caterpillars move down into the understory to feed, often totally defoliating the understory. Understory feeding was not possible in our experimental setup, thus we may see more crowding effects in the cages than would occur naturally. Fig. 6 illustrates the data and estimates of α.

B.2. Parasitism rates: Experimental data and parameter estimation

Parasitized and unparasitized caterpillar densities were estimated using a time-limited cocoon search. The time taken to count 50 cocoons is recorded, to a maximum of 15 min. If 50 cocoons were collected in less than 15 min, then the number that would have been collected in 15 min was calculated. The full details of the method are discussed in Roland and Taylor (1997).

There are no known measurements of the statistical distribution of parasitoid attacks on the forest tent caterpillar. However, for other tachinids (e.g. *Cyzenis albicans* attacking the winter moth), attacks are often clumped (Hassell, 1980; Roland, 1986). We considered two models of parasitism, the negative binomial model for clumped attack ($f(P_t) = (1 + aP_t/\kappa)^{-\kappa}$) and the Poisson model of random searching ($f(P_t) = e^{-aP_t}$).

Parasitism data (H_t, P_t, P_{t+1}) was available for three years (1994–1996). To prevent problems with algorithm convergence data for which $P_{t+1} = H_t$ were removed (1996 data set only). For this reason, we used nonlinear least squares to fit $H_t - P_{t+1} = f(P_t)$ rather than maximum likelihood. For $f(P_t) = (1 + aP_t/\kappa)^{-\kappa}$, estimates of κ and a were not significantly different from 0 (similar results for all three years of data). Fits of $f(P_t) = e^{-aP_t}$ gave values of R^2 ranging from 0.410 to 0.819. As seen in Fig. 5, the spread of the data illustrates that this is not an ideal model of parasitism; however, collection of parasitism data is problematic

and we know of no one who has successfully estimated parasitoid searching efficiency, a, in a field setting. The data lie inside the 95% confidence intervals for the predictions. Since 1994 is a year just prior to an outbreak, the parasitoids are truly searching; the years following this have hosts in such high abundance that a would be underestimated. Using the Poisson model for parasitism and the 1994 data we obtain $a = 0.03$. The 95% confidence interval for this estimate is small, (0.009, 0.0425).

There is some suggestion that the parasitoid *Aleiodes malacosomatus* may have a second generation on a different host at the end of the season. However, as yet this host has not been identified, so we have omitted this complication from the model formulation.

B.2.1. Estimating the parameters of Ricker density-dependence

The data used in the model selection of $\mu(H_t)$ measures H_t in units of "number per leaf cluster", while the parasitism data is measured in units of "cocoon counts". The model requires the same units for H_t and P_t, and we cannot easily convert between cocoon counts and counts per leaf cluster. We can instead directly estimate parameters for $\mu(H_t) = H_t r/K$ using the caterpillar cocoon count data together with data on the defoliation levels.

We assume that hosts reach carrying capacity, K, at 90% defoliation. A choice of 90% defoliation was arbitrary; however, forest tent caterpillar densities must be very close to their carrying capacity when leaf cover has been driven to these very low levels. Using nonlinear least squares we fit a Holling type II function to the data, a reasonable description of the consumer–resource interaction between the caterpillar and their host plant, aspen. The type II function allows us to obtain values for K; estimates were between 210 and 360 cocoons per 15 min. Combining the three years of data (1994–1996) yields an estimate of $K = 260$.

Lastly, we estimate r, the geometric growth rate of the host. Each female forest tent caterpillar lays only one egg mass, typically containing 150–350 eggs (Parry, 1994). Sippell (1957) reported non-parasitoid mortality of the hosts at a level of 98%. Calculations using our data obtained the same estimate of mortality. Thus, assuming a 1:1 sex ratio, $r \approx \ln(150/2 \times 0.02) - \ln(350/2 \times 0.02) \approx 0.4$–1.3. This is consistent with the Berryman (1995) estimates ($r = 0.58$–1.58) for other forest lepidoptera. Using a mean egg mass size of 250, we obtain $r = 0.9$.

B.2.2. Correlation between the host–parasitoid model time series and data

To validate the model we compared the output time series to an independent data set, Hodson's time series for Western Canada (Hodson (1941)). The data classifies each year as local outbreak, general outbreak or no-outbreak. We re-classify this according to the presence (1) or absence (0) of forest tent caterpillar outbreak. The model output is classified in the same way, with host densities above an arbitrary threshold classified as outbreak presence (1), and below the threshold as outbreak absence (0). As the threshold is arbitrary, we classify the model for a range of threshold densities from 30% of host carrying capacity, in increments of 10%, to 80% of host carrying capacity.

To compare the model to the data we use binary correlation coefficients. For each value of α between 0 and 1 we run the model for 1000 time iterations to exclude transients, and then match the end of this time series to the data. We calculate the number A of outbreak matches, where the model and data both show an outbreak for a given year; we also calculate the number of non-outbreak matches D, and non-matches $(B + C)$. The binary correlation coefficient ρ is the proportion of matches ($\rho = \frac{A+D}{A+D+B+C}$).

When matching the model and data we phase-shift the model until we have maximized ρ for a given α, to ensure that the data

and model are in phase when we match the first time point. We found that correlation between the model and data is maximized for $\alpha \approx 0.35$ (see Fig. 3). Hodson's times series data is for 23 regions in the US and Canada from 1886 to 1940. Table 2 details the mean period, outbreak duration and non-outbreak duration for nine locations. The remaining 14 sites from Hodson's study indicated only one complete outbreak during the course of the study and were therefore omitted.

Appendix C. The coexistence of an early and a late emerging parasitoid

We consider a special case of Eqs. (11) where $\alpha_P = 1, \alpha_Q = 0$, $\phi = 0$ and $\kappa \to \infty$ and $\mu(H_t) = rH_t/K$. Scaling the equations such that $H_t = Kh_t, P_t = a_P p_t$ and $Q_t = a_Q q_t$ gives,

$$h_{t+1} = h_t e^r e^{-rh_t} e^{-p_t} e^{-q_t}, \qquad p_{t+1} = a_P Kh_t e^{-rh_t}(1 - e^{-p_t})e^{-q_t}$$

and $\quad q_{t+1} = a_Q Kh_t(1 - e^{-q_t})$.

We show that coexistence of an early and late emerging parasitoid cannot occur when the searching efficiency of the late parasitoid (p_t) is less than or equal to that of the early parasitoid (q_t).

Claim 1. *Suppose* $h_{\max} > h_0 > 0$ *and* $0 < p_0 \leq q_0$ *then* $h_t < h_{\max}$ *for all* $t \geq 0$, *where* $h_{\max} = \frac{1}{r}e^{r-1}$.

Proof.

$$h_1 = h_0 e^{r(1-h_0)}e^{-p_0}e^{-q_0} < h_0 e^{r(1-h_0)} < \frac{1}{r}e^{r-1},$$

since $h_0 e^{r(1-h_0)}$ has a maximum at $h_0 = 1/r$. $\quad\square$

Claim 2. *Suppose* $a_P \leq a_Q$, $h_0 > 0$ *and* $0 < p_0 \leq q_0$ *then* $p_t < q_t$ *for all* $t \geq 0$.

Proof. Using proof by induction, for $t = 1$

$$\frac{p_1}{q_1} = \left(\frac{1 - e^{-p_0}}{1 - e^{-q_0}}\right)e^{-q_0}\frac{a_P}{a_Q}e^{-rh_0} < 1.$$

The inductive assumption holds for $t = k$. We now show $\frac{p_t}{q_t} < 1$ for $t = k + 1$.

$$\frac{p_{k+1}}{q_{k+1}} = \left(\frac{1 - e^{-p_k}}{1 - e^{-q_k}}\right)e^{-q_k}\frac{a_P}{a_Q}e^{-rH_k} < 1. \quad\square$$

Claim 3. *Suppose* $a_P \leq a_Q$, $h_0 > 0$ *and* $0 < p_0 \leq q_0$ *then* $p_t \to 0$ *as* $t \to \infty$.

Proof. 1. We first show that if $p_k < q_k$ then $\frac{1-e^{-p_k}}{e^{q_k}-1} < \frac{p_k}{q_k}$.

$$\frac{1 - e^{-p_k}}{e^{q_k} - 1} - \frac{p_k}{q_k} = \frac{p_k - \frac{p_k^2}{2!} + \frac{p_k^3}{3!} - \cdots}{q_k + \frac{q_k^2}{2!} + \frac{q_k^3}{3!} + \cdots} - \frac{p_k}{q_k}$$

$$= \frac{-\frac{p_k^2}{2!}(p_k + q_k) - \frac{p_k^3}{3!}(q_k^2 + p_k^2) - \cdots}{e^{q_k} - 1} < 0.$$

2. Using Claim 2 we know that $p_k < q_k$ so part 1 above holds. Hence, $R_k = \frac{p_k}{q_k}$ satisfies

$$R_{k+1} < R_k\frac{a_P}{a_Q}e^{-rh_k} < R_k\frac{a_P}{a_Q}.$$

Hence, $R_k < R_0\left(\frac{a_P}{a_Q}\right)^k \to 0$ as $k \to \infty$.

3. By Claim 1 $h_t \leq h_{\max}$ and therefore $q_t \leq a_Q Kh_{\max} = q_{\max}$. By part 2 above we have $\frac{p_k}{q_{\max}} \leq \frac{p_k}{q_k} \to 0$ as $k \to \infty$ and hence $p_k \to 0$ as $k \to \infty$.

In conclusion, for p_t to persist with q_t we require that $a_P \geq a_Q$. $\quad\square$

References

Akaike, H., 1974. A new look at statistical model identification. IEEE Transactions on Automatic Control AU. 19, 716–722.

Anon, Summer, 1991. Forest insect and disease survey conditions in Ontario. Forestry Canada Survey Bulletin.

Astrom, M., Lundberg, P., Lundberg, S., 1996. Population dynamics with sequential density-dependence. Oikos 75 (2), 174–181.

Beddington, J.R., Free, C.A., Lawton, J.H., 1975. Dynamic complexity in predator–prey models framed in difference equations. Nature 255, 58–60.

Bellows, T.S., 1981. The descriptive properties of some models for density dependence. Journal of Animal Ecology 50 (1), 139–156.

Berryman, A.A., 1995. Population cycles of the maternal and allometric hypotheses. Journal of Animal Ecology 64.

Berstein, C., 1986. Density dependence and the stability of host–parasitoid systems. Oikos 47, 176–180.

Bonsall, M.B., Godfray, H.C.J., Briggs, C.J., Hassell, M.P., 1999. Does host self-regulation increase the likelihood of insect-pathogen population cycles? American Naturalist 153 (2), 228–235.

Briggs, C.J., 1993. Competition among parasitoid species on a stage-structured host, and its effect on host suppression. American Naturalist 141, 372–397.

Briggs, C.J., Nisbet, R., Murdoch, W., 1993. Coexistence of competing parasitoid species on a host with a variable life cyle. Theoretical Population Biology 44, 341–373.

Briggs, C.J., Sait, S.M., Begon, M., Thompson, D.I., Godfray, H.C.J., 2000. What causes generation cycles in populations of store-product moths? Journal of Animal Ecology 69, 352–366.

Cameron, T.C., Wearing, H.J., Rohani, P., Sait, S.M., 2005. A koinobiont parasitoid mediates competition and generates additive mortality in healthy host populations. Oikos 110, 620–628.

Cooke, B.J., 2001. Interactions between climate, trembling aspen, and outbreaks of forest tent caterpillar in Alberta. Ph.D. Thesis. University of Alberta.

Cooke, B.J., Lorenzetti, F., 2006. The dynamics of forest tent caterpillar outbreaks in Québec, Canada. Forest Ecology and Management 226, 110–121.

Dwyer, G., Dushoff, J., Yee, S.H., 2004. The combined effects of pathogens and predators on insect outbreaks. Nature 430, 341–345.

Getz, W.M., 1996. A hypothesis regarding the abruptness of density dependence and the growth rate of populations. Ecology 77 (7), 2014–2026.

Godfray, H.C.J., Waage, J.K., 1991. Predictive modeling in biological control: The mango mealybug (*Rastrococcus invadens*) and its parasitoids. Journal of Applied Ecology 28, 434–453.

Gurney, W.S.C., Nisbet, R.M., Lawton, J.H., 1983. The systematic formulation of tractable single-species population models incorporating age structure. Journal of Animal Ecology 52 (2), 479–495.

Haldane, J.B.S., 1949. Disease and evolution. Symposium sui fattori ecologici e genetici della speciazone negli animali. Ricerca Scientifica 19 (Suppl.), 3–11.

Hassell, M.P., 1978. The Dynamics of Arthropod Predator–Prey Systems. Princeton University Press, Princeton, NJ.

Hassell, M.P., 1980. Foraging strategies, population models and biological control: A case study. Journal of Animal Ecology 49, 603–628.

Hassell, M.P., 2000. Host–parasitoid population dynamics. Journal of Animal Ecology 69, 543–566.

Hodson, A.C., 1941. An ecological study of the forest tent caterpillar, *Malacosoma disstria* Hbn., in Northern Minnesota. Tech. Rep. 148. University of Minnesota Agricultural Station Technical Bulletin.

Hogarth, W.L., 1984. Interspecific competition in larvae between entomophagous parasitoids. American Naturalist 124 (4), 552–560.

Lane, S.D., Mills, N.J., 2003. Intraspecific competition and density dependence in an *Ephestia kuehniella–Venturia camescens* laboratory system. Oikos 101, 578–590.

May, R.M., 1978. Host–parasitoid systems in patchy environments: A phenomenological model. Journal of Animal Ecology 47 (3), 833–844.

May, R.M., Hassell, M.P., Anderson, R.M., Tonkyn, D.W., 1981. Density dependence in host–parasitoid models. Journal of Animal Ecology 50 (3), 855–865.

Murdoch, W.W., Kendall, B.E., Nisbet, R.M., Briggs, C.J., McCauley, E., Bolser, R., 2002. Single-species models for many-species food webs. Nature 417, 541–543.

Neubert, M.G., Kot, M., 1992. The subcritical collapse of predator populations in discrete-time predator–prey models. Mathematical Bioscience 10, 45–66.

Nicholson, A.J., Bailey, V.A., 1935. The balance of animal populations. Part 1. Proceedings of the Zoological Society, London 1935, 551–598.

Parry, D., 1994. The impact of predators and parasitoids on natural and experimentally created populations of forest tent caterpillar, *Malacosoma disstria* Hubner (Lepidoptera: Lasiocampidae). Master's Thesis. University of Alberta, Edmonton, Alberta.

Parry, D., 1995. Larval and pupal parasitism of the forest tent caterpillar, *Malacosoma disstria* Hubner (Lepidoptera: Lasiocampidae), in Alberta Canada. Canadian Entomologist 127, 877–893.

Rodriguez, D.J., 1988. Models of growth with density regulations in more than one life stage. Theoretical Population Biology 34, 93–117.

Roland, J., 1986. Parasitism of winter moth in British Columbia during build-up of its parasitoid Cyzenis albicans: Attack rate on oak versus apple. Journal of Animal Ecology 55, 215–234.

Roland, J., Mackey, B.G., Cooke, B., 1998. Effects of climate and forest structure on duration of forest tent caterpillar outbreaks across Central Ontario, Canada. Canadian Entomologist 130, 703–714.

Roland, J., Taylor, P., Cooke, B., 1997. Forest structure and the spatial pattern of parasitoid attack. In: Forests and Insects. Chapman and Hall, London, pp. 97–106.

Roland, J., Taylor, P.D., 1997. Insect parasitoid species respond to forest structure at different spatial scales. Nature 386, 710–713.

Sippell, W.L., 1957. A study of the forest tent caterpillar *Malacosoma disstria* Hbn., and its parasite complex in Ontario. Ph.D. Thesis. University of Michigan.

Sippell, W.L., 1962. Outbreaks of the forest tent caterpillar, *Malacosoma disstria* Hbn., a periodic defoliator of broad leaf trees in Ontario. Canadian Entomologist 94, 408–416.

Sisterson, M.S., Averill, A.L., 2003. Interactions between parasitised and unparasitised conspecifics: parasitoids modulate competitive dynamics. Oecologia 135, 362–371.

Spataro, T., Bernstein, C., 2004. Combined effects of intraspecific competition and parasitoid attacks on the dynamics of a host population. 1. A stage structured model. Oikos 105, 148–158.

Taylor, A.D., 1997. Density-dependent parasitoid recruitment per parasitised host: Effects on parasitoid–host dynamics. American Naturalist 149 (5), 989–1000.

Umbanhowar, J., Hastings, A., 2002. The impact of resource limitation and the phenology of parasitoid attack on the duration of insect herbivore outbreaks. Theoretical Population Biology 62, 259–269.

Varley, G.C., Gradwell, G.R., 1960. Key factors in population studies. Journal of Animal Ecology 29, 399–401.

Wang, Y.H., Gutierrez, A.P., 1980. An assessment of the use of stability analyses in population ecology. Journal of Animal Ecology 49, 435–452.

Wearing, H.J., Sait, S.M., Cameron, T.C., Rohani, P., 2004. Stage-structured competition and the cyclic dynamics of host–parasitoid populations. Journal of Animal Ecology 73, 706–722.

White, S.M., Sait, S.M., Rohani, P., 2007. Population dynamic consequences of parasitised-larval competition in stage-structured host–parasitoid systems. Oikos 116, 1171–1185.